KITP Friction, Fracture and Earthquake Physics Conf., Santa Barbara, 15-19 Aug 2005

Structure of Mature Faults and Physics of Their Weakening During Earthquakes

James R. Rice (Harvard)

Collaborators on related studies:

Rachel E. Abercrombie (Boston Univ.)
Massimo Cocco (INGV, Rome)
Laurent M. Jacques (Ecole Poly. & Corps des Mines)
Nadia Lapusta (Caltech)
Alan W. Rempel (Univ. of Oregon)
John W. Rudnicki (Northwestern Univ.)
Charles G. Sammis (Univ. So. Calif.)
Paul Segall (Stanford)
Victor Tsai (Harvard)

Principal references and download links

J. R. Rice, "Heating and weakening of faults during earthquake slip", submitted to *J. Geophys. Res.*, Aug. 2005.
http://esag.harvard.edu/rice/Rice_heat_weaken_toJGR05.pdf

J. R. Rice and M. Cocco, "Seismic fault rheology and earthquake dynamics", in *The Dynamics of Fault Zones*, ed. M. R. Handy, Dahlem Workshop (Berlin, January 2005) Report 95, The MIT Press, Cambridge, MA, publication expected 2006.
http://esag.harvard.edu/rice/216_RiceCocco_DahlemWrkshp05.pdf

J. R. Rice, C. G. Sammis and R. Parsons, "Off-fault secondary failure induced by a dynamic slip-pulse", *Bull. Seismol. Soc. Amer.,* **95** (1), pp. 109-134, doi: 10.1785/0120030166, 2005.
http://esag.harvard.edu/rice/211_RiceSammisPars_BSSA05.pdf

R. E. Abercrombie and J. R. Rice, "Can observations of earthquake scaling constrain slip weakening?", *Geophys. J. Int.*, **162**, pp. 406-424, doi: 10.1111/j.1365-246X.2005.02579.x, 2005.
http://esag.harvard.edu/rice/212_AbercrombieRice_GJI05.pdf

CHESTER ET AL.: INTERNAL STRUCTURE OF THE SAN ANDREAS FAULT *J.Geophys. Res.* (1993) 773

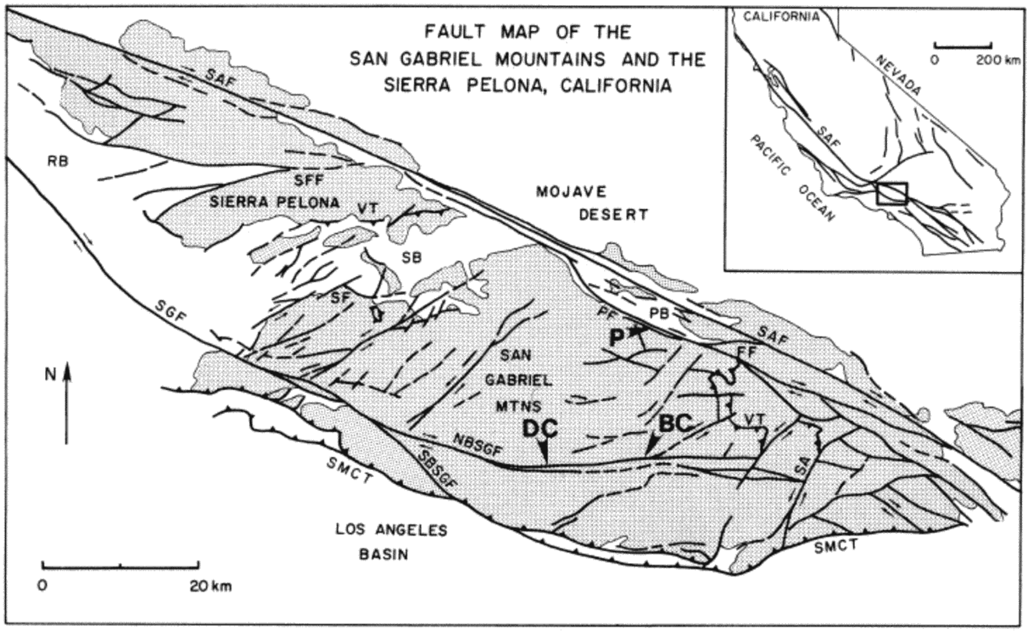

Fig. 1. Generalized geologic map of the San Gabriel Mountains and vicinity, southern California. Stippled pattern represents crystalline rocks. Bold arrows indicate the study localities discussed in the text: Devil's Canyon (DC), Bear Creek (BC), and Punchbowl (P). Key: active trace of the San Andreas fault (SAF), San Gabriel fault (SGF), North Branch San Gabriel fault (NBSGF), South Branch San Gabriel fault (SBSGF), Punchbowl fault (PF), Sierra Madre-Cucamonga thrust (SMCT), San Antonio fault (SA), Vincent thrust (VT), Fenner fault (FF), Soledad fault (SF), San Francisquito fault (SFF), Ridge basin (RB), Soledad basin (SB) and Punchbowl basin (PB).

F. Chester, J. Evans and R. Biegel, *J. Geoph. Res.,* **98** (B1), 771-786 (1993)

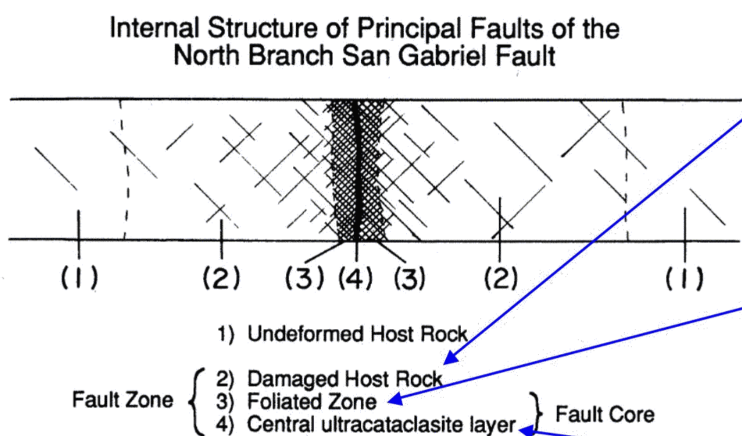

30-100 m
(Damage ≈ *highly cracked rock*.
Zone with macro faults or fractures extends ~ 10x further.)

1-10 m
(Sometimes described as *foliated gouge*, or for some faults, simply as *gouge*.)

10s-100s mm
(But ***principal failure surface*** is *much thinner*, typically < 1-5 mm!)

Fig. 2. Schematic section across the North Branch San Gabriel fault zone illustrating position of the structural zones of the fault. The diagram is not to scale.

Chester, F. M., and J. S. Chester, Ultracataclasite structure and friction processes of the Punchbowl fault, San Andreas system, California, *Tectonophysics*, **295** (1-2): 199-221,1998

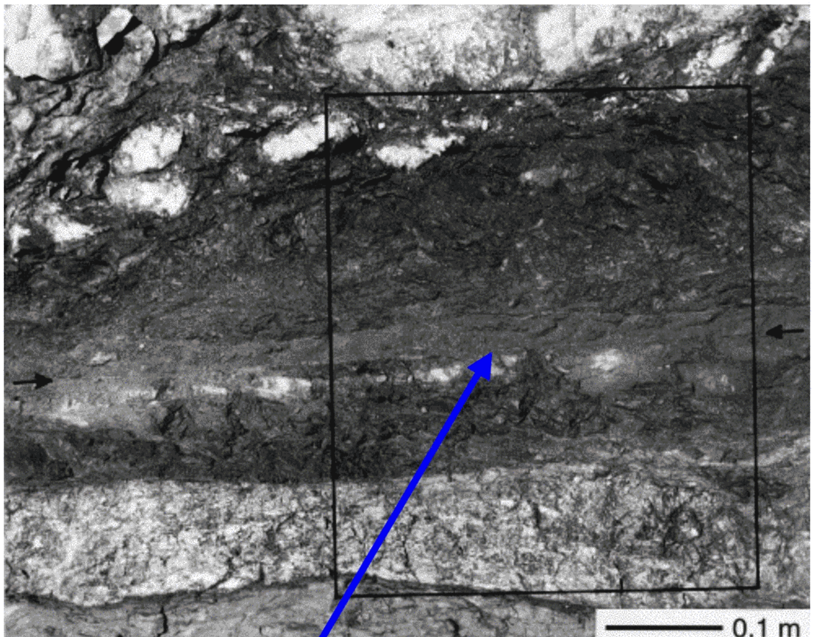

Prominent slip surface (pss) is located in the center of the layer and identified by the black arrows. (Exhumed from 2-4 km depth. Total slip ≈ 44 km. "Several km" of slip in earthquakes on the pss.)

From J. S. Chester and D. L. Goldsby, *SCEC Ann. Rpt*., 2003 (also, Chester et al., *EOS*, *Trans AGU*, 2003)

Punchbowl Fault prominent slip surface

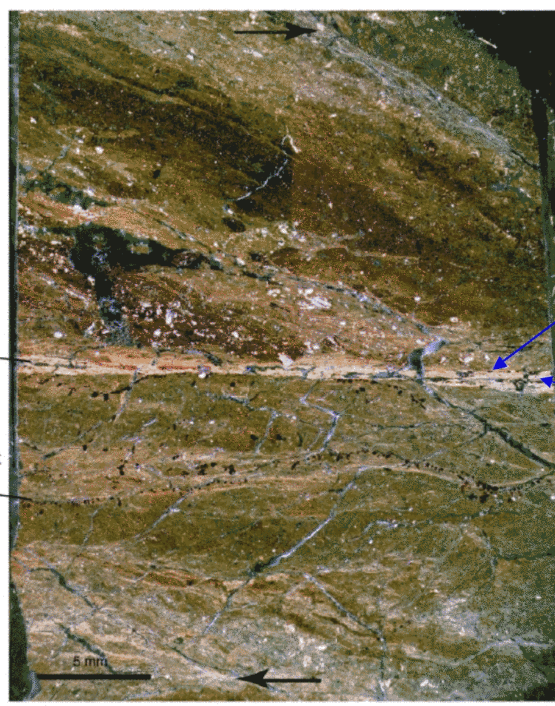

Figure 2. Photomosaic of entire thin section 1b (see Figure 1) under cross-polarized light showing the pss between the cohesive and less cohesive yellow-brown ultracataclasite. The pss is distinguished by uniform birefringence within a narrow planar band having sharp boundaries. Note the presence of relict pss and truncation of layering at the pss.

Median Tectonic Line Fault (MTL), Japan

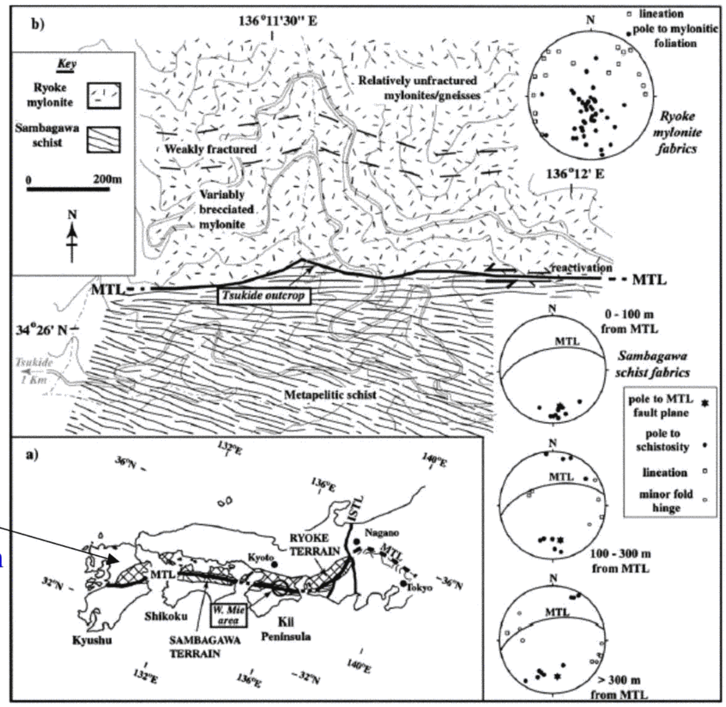

Fig. 1. (a) The Median Tectonic Line (MTL) and adjacent tectonic units in SW Japan. ISTL denotes the Itoigawa–Shizuoka Tectonic Line. (b) Geological map of the Median Tectonic Line near Tsukide, western Mie Prefecture, including structural data on the deformation fabrics around the Median Tectonic Line. The stereograms are lower-hemisphere equal-area stereographic projections.

Median Tectonic Line Fault, Japan

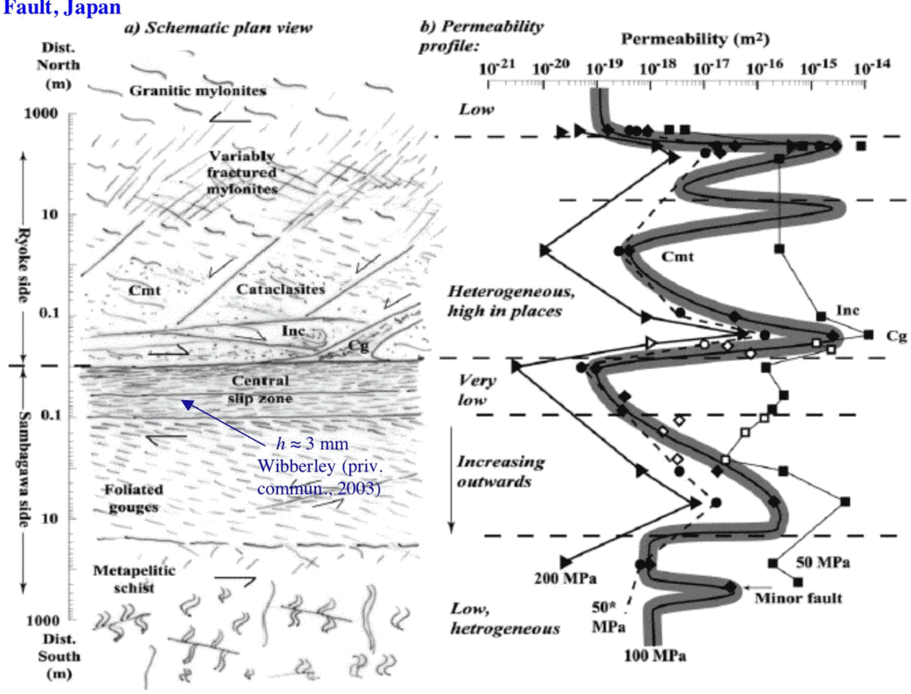

Fig. 11. Sketch summary of the main elements of permeability structure across the Median Tectonic Line. (a) Summary of the structural zones; (b) summary permeability data distribution for different confining pressures (stated at the base, with * denoting data from the deconfining path), for 20 MPa pore pressure, given the mapped distribution of fault rocks shown in Figs. 1–3. Note that the distance axis is logarithmic in both directions away from the Ryoke/Sambagawa contact. 'Cmt' and 'Inc' denote cemented and incohesive foliated cataclasites, respectively, and 'Cg' denotes crenulated gouge.

(Wibberley and Shimamoto, *JSG*, 2003) permeability of clay gouge containing the central slip zone, Median Tectonic Line Fault, Japan

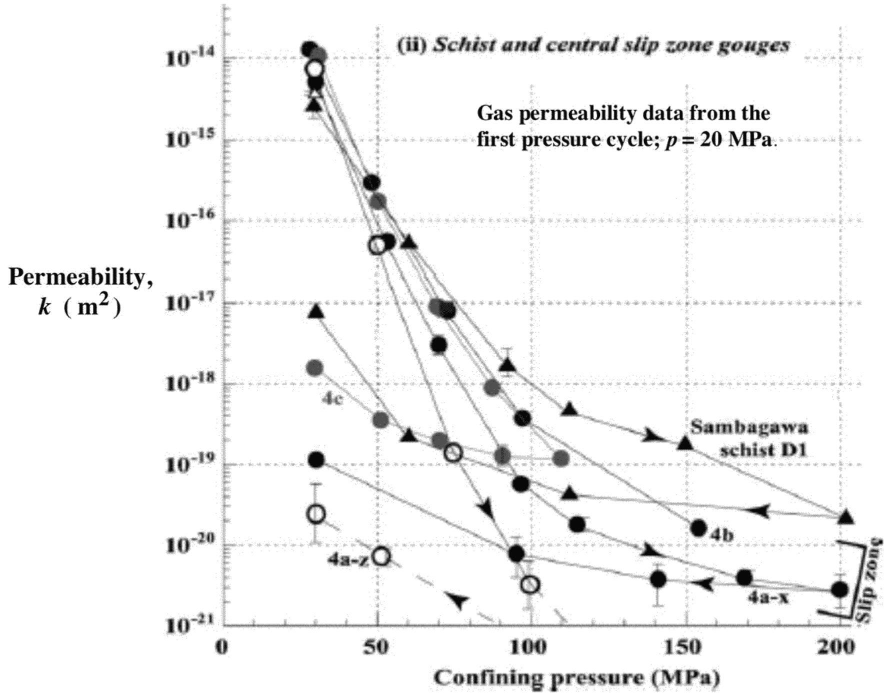

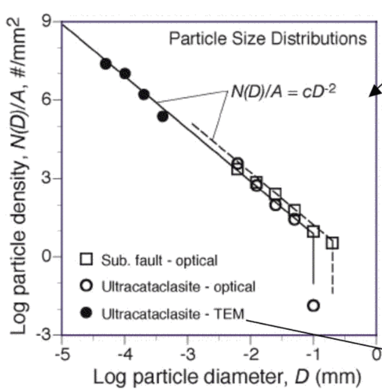

Particle size distribution for ultracataclasite hosting the Punchbowl pss (Chester et al., *Nature*, subm. 2005):

- $N(D)/A$ (= number of particles per unit sample area with $2D/3 <$ diameter $< 4D/3) \approx c/D^2$.
- Implies $n_V(D) \propto 1/D^4$ for 10-30 nm $< D <$ 70 μm.
- D_{50}(= size such that 50% by wt. is larger) ≈ 1 μm.
- *If* standard granular material guidelines hold, thinnest possible shear zone thickness is ~ 10-20 μm.
- But D = 10 μm corresponds to D_{20} to D_{25}! (also, clumping)

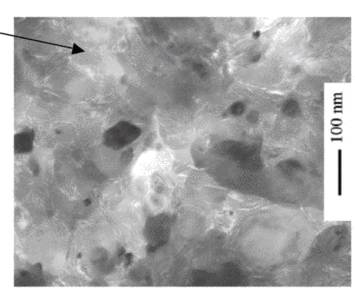

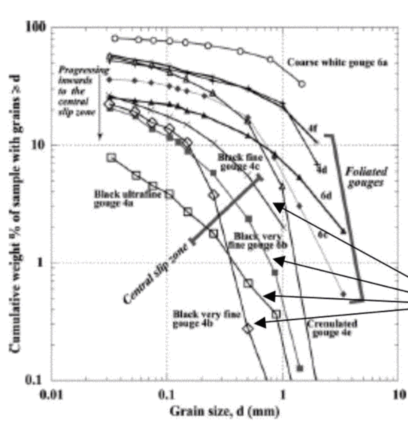

Comparison, size distribution for ultracataclasite hosting the MTL pss (Wibberley & Shimamoto, 2003):

- Extrapolating, $D_{50} <$ 10 μm and D = 10 μm corresponds to ~ D_{20} to D_{30}

Compare, faults with > 5,000 large-slip earthquakes on previous slides vs. a fault with 1 earthquake (a fresh rupture) here

Fresh rupture in a M=3.7 earthquake at 2 km depth, 1997, due to mining operations in the Hartebeestfontein gold mine, South Africa.

Formed the *Bosman* fault within otherwise unfaulted quartzitic layers.

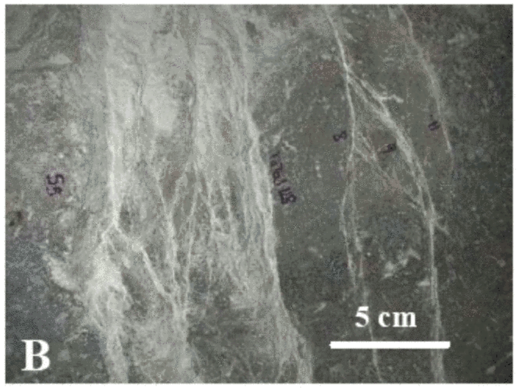

[Wilson, Dewers, Reches & Brune, *Nature*, 2005]

• 100 m long. • At least 5 m wide. • 0.4 m maximum slip.
• Contains 4-6 large, subparallel segments with hundreds of secondary, small fractures.

If rupture on major faults (usually) takes place in a narrow fault core, why are there wide granulated and damaged zones?

Perspective 1, Large-scale geological view:

• Major faults start their lives as independent, disconnected and poorly aligned fault segments (e.g., Pollard & Segall).

The active locus smooths with slip (e.g., fewer step-overs per unit length, Wesnousky et al.).

Broad zones affected by prior faulting give way to narrower channels of continuing activity.

• Major fault traces, while smooth in the direction of slip, do have fractal-distributed Irregularities (Power and Tullis).

The more they slip the broader a zone which must be activated to accommodate the misfits.

Perspective 2, Processes in individual events:

• The rupture front concentrates stress over a wide zone, the more so the more rapid the propagation speed v_r.

[Rice, Sammis & Parsons (*BSSA*, 2005), based on Broberg (*GJRAS,* 1978; *book*, 1999), Freund (*JGR*, 1979), Heaton (*EPSL,* 1990), & Poliakov, Dmowska & Rice (*JGR,* 2002)]

(blue arrow) denotes parameter estimated from seismic slip inversion, Heaton (1990) -- L, δ and v_r

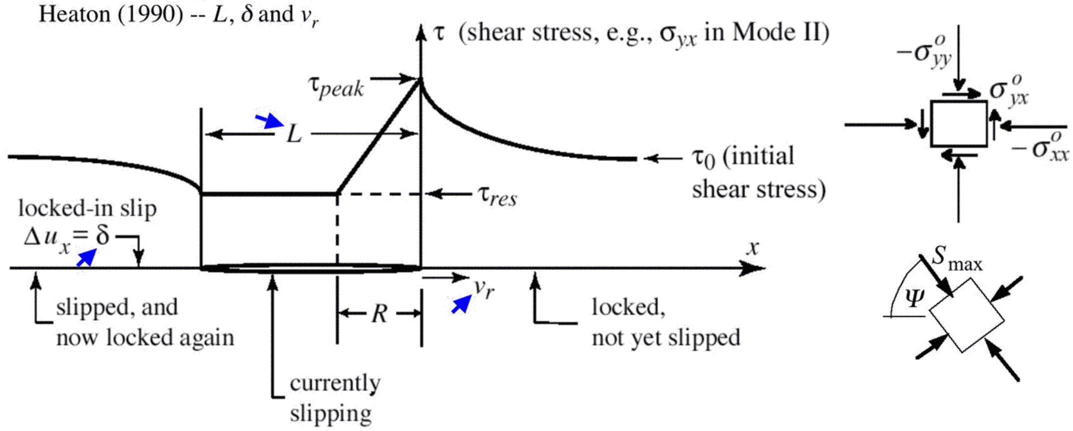

To formulate as an elasticity problem for a steady-state field, dependent on $x - v_r\, t$ and y, we specify:

$$v_r\ ,\ L\ ,\ \delta\ ,\ \frac{\tau_{peak}}{-\sigma_{yy}^{o}}\ ,\ \frac{\tau_{res}}{\tau_{peak}}\ ,\ \Psi \text{ and one of } \frac{R}{L} \text{ or } \frac{\tau_0 - \tau_{res}}{\tau_{peak} - \tau_{res}}\ .$$

from Heaton (1990) (v_r, L, δ); $f_{peak} \approx 0.6$; e.g., 0.2

Procedure:

(1) Solve the 2D elasticity problem, calculate stresses $\sigma_{\alpha\beta}$.

(2) Check if the $\sigma_{\alpha\beta}$ would cause Coulomb *shear failure* [$\tau > (-\sigma_n)$x tan(31°)] on some Orientation, or cause *tensile failure* [$\sigma_2 > 0$].

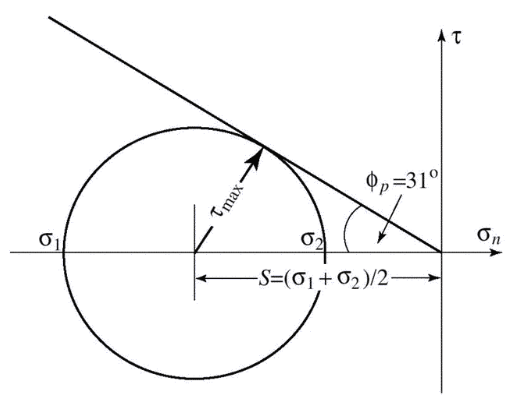

[Rice et al. (*BSSA*, 2005), building on Poliakov et al. (*JGR*, 2002)]

For $R/L = 0.1$, and $\tau_r / \tau_p = 0.2$ (nearly complete strength loss)

YELLOW = shear failure **RED = tensile failure**

Poroelastic effects included; Skempton $B = 0.6$ $[\Delta p = -B\, \Delta(\sigma_{11} + \sigma_{22} + \sigma_{33})/3]$

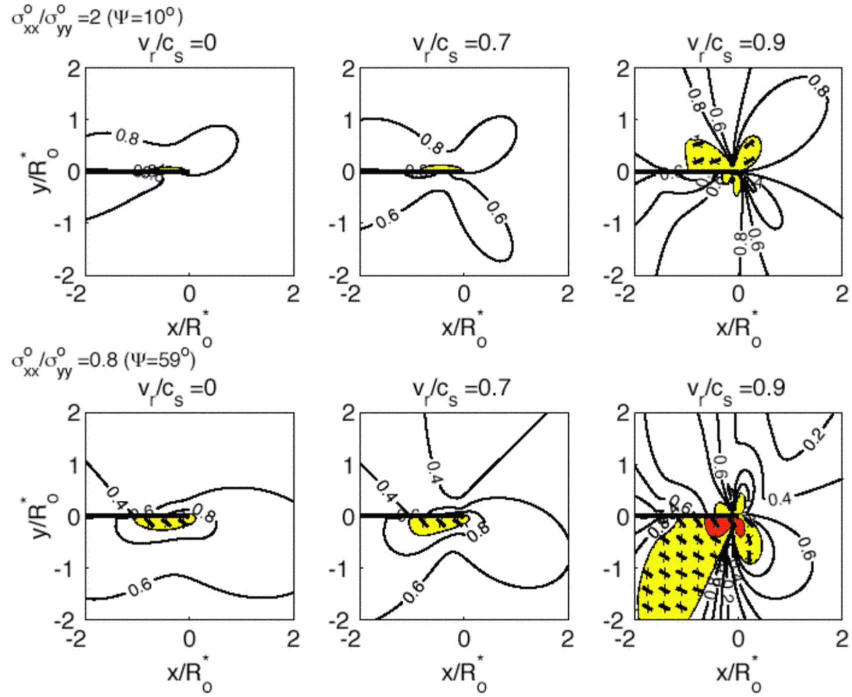

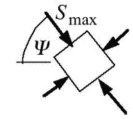

Scale length in plots:

$(R_o^*)_{avg} = 20\text{-}30$ m,

$R_o^* = 1\text{-}70$ m,

fitting model to Heaton (1990) earthquake set, assuming $f_p = 0.6$ and hydrostatic initial pore pressure.

Correlation with natural examples

(Poliakov, Dmowska and Rice, *JGR*, 2002)

Depth cross-section view: **Shallow S_{max} direction, $\Psi \approx 12\text{-}18^o$**; secondary failures on ***compressional*** side:

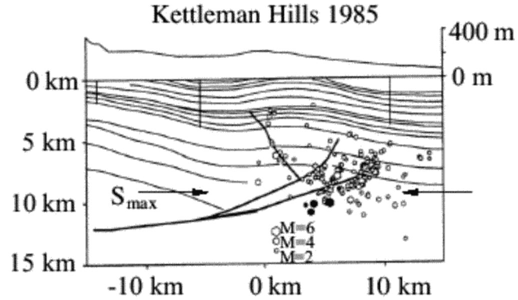

(Ekstrom et al., 1992; fault locations from Meltzer, 1989)

Map view: **Steep S_{max} direction, $\Psi \approx 60^o$**; secondary failures on ***extensional*** side:

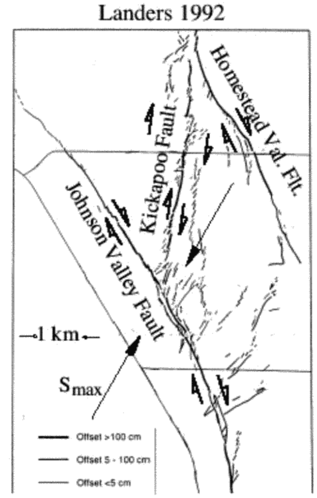

(fault map from Sowers et al., 1994; stress from Hardebeck and Hauksson, 2001)

Physics of Fault Zone Processes during Seismic Slips

Questions:

• How does *shear stress* (τ) vary with *slip* (δ) during earthquakes?
Focus is on *weakening* during *rapid, large* slip δ on mature faults, i.e., δ >> 0.01-0.1 mm (the slip range at which earthquakes are thought to *nucleate*, according to rate & state concepts and lab-based properties).

• What are the *physical mechanism* of weakening during slip?
Suggested here: Primary mechanisms are
- ***Thermal pressurization of pore fluid,*** and
- ***Flash heating at highly stressed frictional contacts.***

Both seem to be important.
At *sufficiently large slip*, others mechanisms become important:
- ***Melting*** if large enough normal stress (deeper slip),
- ***Gel formation*** in lithologies of high silica content.

• What *fracture energy* (G) is implied by the τ *vs*. δ relation?
Important because we can thereby *test* any proposed τ *vs*. δ against *seismic* constraints on G.

Background for theoretical modeling of stress vs. slip relation:

Field and lab observations, exposures of ***mature, highly slipped*** fault zones:

• Slip in *individual events* is localized to a *thin shear zone* (h < 1-5 mm) within a *finely granulated* (*ultracataclastic,* possibly *clayey*) fault core that is of order 10s to 100s mm thickness, with low permeability(estimated $k \sim 10^{-20}$ m^2 at mid-seismogenic depths)

[that despite the existence of *much wider* (~1-100 m) *damage zones* with granulation, pervasive cracking and/or minor faulting]

Hypotheses:

• Earthquake failure occurs in a *water-saturated* fault zone (a porous granular material in the shallow to middle crust).

• It has *material properties* (permeability, porosity, poroelastic moduli) like those inferred from *lab studies of fault materials* from the *Median Tectonic Line* (*MTL*), *Nojima* and *Hanaore* faults in Japan.

[locations for which relatively complete data exists]

Frictional weakening by flash heating

[Rice, *EOS, Trans. AGU*, 1999; Beeler & Tullis, *USGS OFR*, 2003]

Flash Heating at Asperity Contacts and Rate-Dependent Friction

Flash heating at frictional asperity contacts:

Suggested in tribology as the key to understanding the slip rate dependence of dry friction in metals at high rates:

Bowden and Thomas, *Proc. Roy. Soc.*, 1954
Ettles, *J. Tribol.*, 1986
Lim and Ashby, *Acta Met.*, 1987
Molinari et al., *J. Tribol.*, 1999

T_f = average temperature along a sliding fault zone (evolves gradually with t compared to much shorter time scale of heating at asperity contacts)

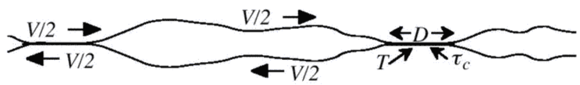

T = local, highly transient, temperature at an asperity contact from flash heating during its brief lifetime θ.
(θ = contact lifetime D/V, D = contact size, V = slip rate).

τ_c = contact shear strength, temperature dependent:

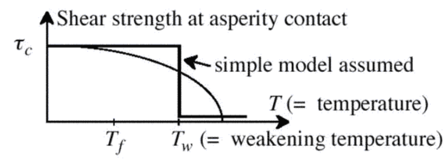

Weakening velocity V_w : When $V > V_w$, asperity of size D weakens ($T \to T_w$, and contact strength $\to$ small value $\tau_{c,w}$) *before* end of contact lifetime D/V :

$$V_w = \frac{\pi \alpha_{th}}{D} \left[\frac{\rho c (T_w - T_f)}{\tau_c} \right]^2$$

Example :

$$\alpha_{th} = 0.5 \text{ mm}^2/\text{s}, \ \rho c = 2.7 \text{ MJ/m}^3\text{K},$$
$$D = 5 \ \mu\text{m}, \ T_w = 900^\circ\text{C}, \ T_f = 20^\circ\text{C}$$
$$\text{and } \ \tau_c = 0.1 \times (\text{elastic shear modulus}) = 3.0 \text{ GPa}$$
$$\Rightarrow \ V_w \approx 0.20 \text{ m/s} \ \ (\approx 0.12 \text{ m/s at } T_f = 200^\circ\text{C})$$

Fits to Tullis & Goldsby [2003] data (quartzite, granite, feldspar, gabbro, calcite) :
V_w = (0.14, 0.14, 0.28, 0.11, 0.27) m/s

Simple model for friction coefficient ("steady state" value in rate & state sense) :

$$f = \begin{cases} f_o & \text{for } 0 < V < V_w \\ f = (f_o - f_w)\dfrac{V_w}{V} + f_w & \text{for } V > V_w \end{cases}$$

where $f_w = f_o \tau_{c,w} / \tau_c << f_o$

Fits to Tullis & Goldsby [2003] data, V = 0 to 0.36 m / s (quartzite, granite, gabbro) :
f_o = (0.64, 0.82, 0.88) , f_w = (0.12, 0.13, 0.15)

from T. E. Tullis and D. L. Goldsby, *SCEC Ann. Rpt.*, 2003

Arkansas Novaculite (Quartzite)

[rotary shear, 1.2 mm slow pre-slip (10 µm/s), then 45 mm of *fast* slip]

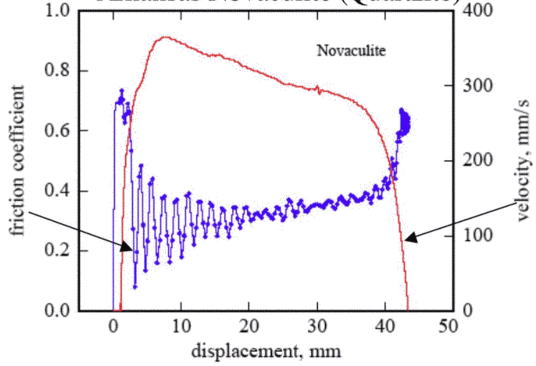

Figure 1- Plot of friction coefficient (in blue) and sliding velocity (in red) vs. displacement for novaculite. At low speeds, friction obtains values of ~0.65. At high speeds up to 0.36 m/s, friction obtains values as low as ~0.3. After fast sliding, friction returns to ~0.65 at low sliding velocities.

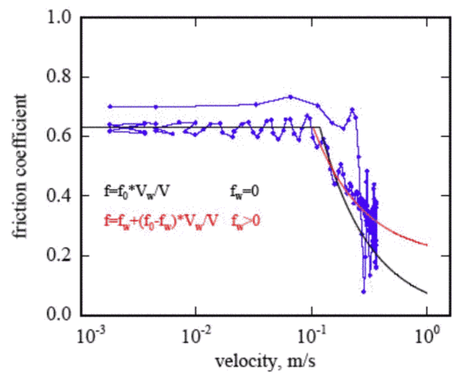

Figure 3- Data from Fig. 1 plotted vs. velocity on a logarithmic scale. Data have been fit with the flash melting equations of *Rice* [1999] (in black) and *Beeler* [unpublished manuscript] (in red), which describe the effect of flash melting on the friction coefficient *f* as a function of sliding velocity. The Rice analysis assumes that melted asperities have zero strength, whereas Beeler's analysis assumes melted asperities have finite strength.

from T. E. Tullis and D. L. Goldsby, *SCEC Ann. Rpt.*, 2003

Also seen in Granite, Tanco Feldspar & Gabbro, but just weakly/ambiguously in Calcite.

Westerly Granite

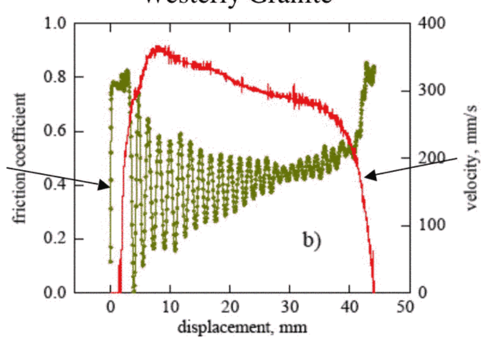

Gabbro (of Tsutsumi & Shimamoto)

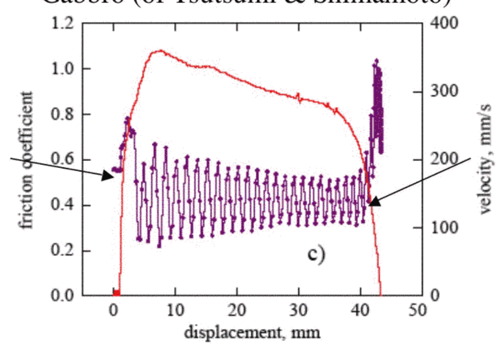

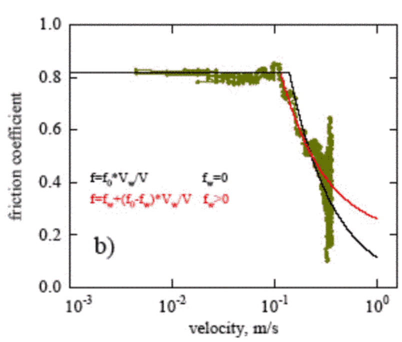

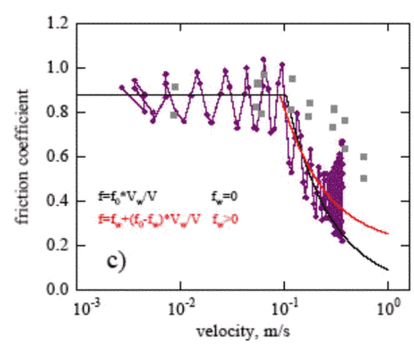

from Vikas Prakash, *SCEC Ann. Mtg.*, 2004

Schematic illustration of the torsional Kolsky bar apparatus

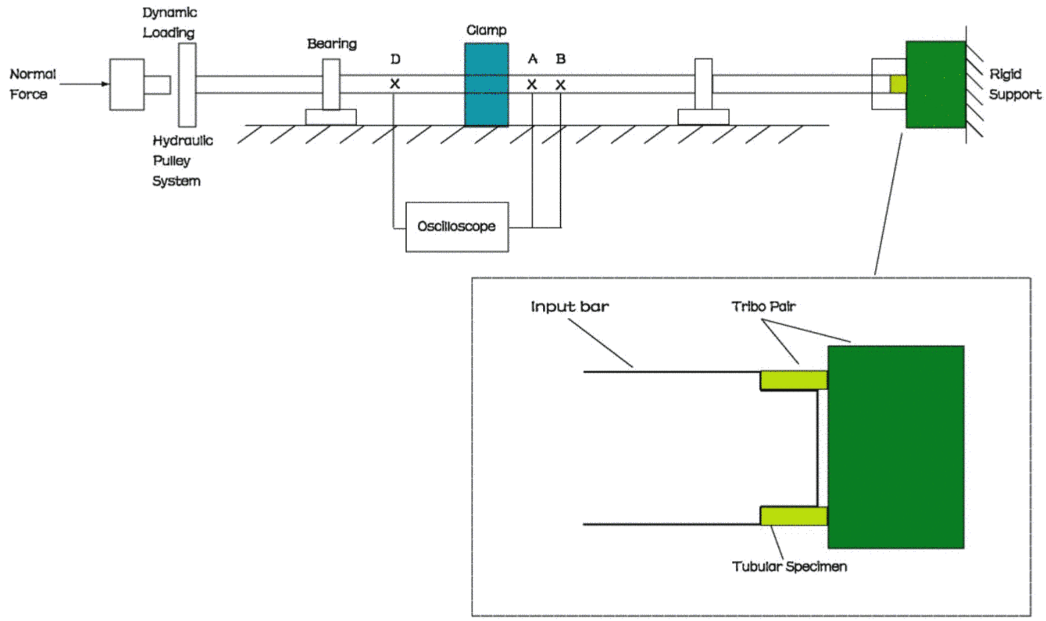

Weakening of friction coefficient *f* at high slip rates

Results here for ***Arkansas novaculite*** (~100% ***quartzite***), determined in rotating annular specimens

Tullis and Goldsby (2003a,b), up to 0.36 m/s

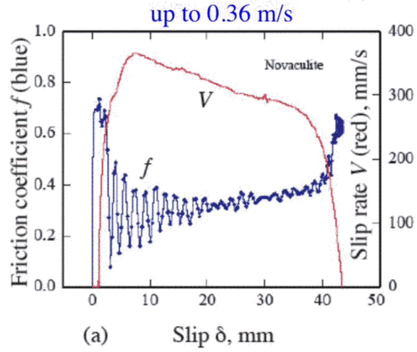

Slip rates V up to 0.36 m/s imposed in Instron testing frame for 45 mm slip, after 1.2 mm pre-slip at ~10 μm/s. At low V, friction coefficient $f \approx 0.65$, whereas at $V > 0.3$ m/s, $f \approx 0.3$.

Comparable rate-weakening was found for ***granite***, ***Tanco albite*** (~100% ***feldspar***), and ***gabbro***, but ambiguous results for ***calcite***.

Prakash (2004), 2 to 4 m/s

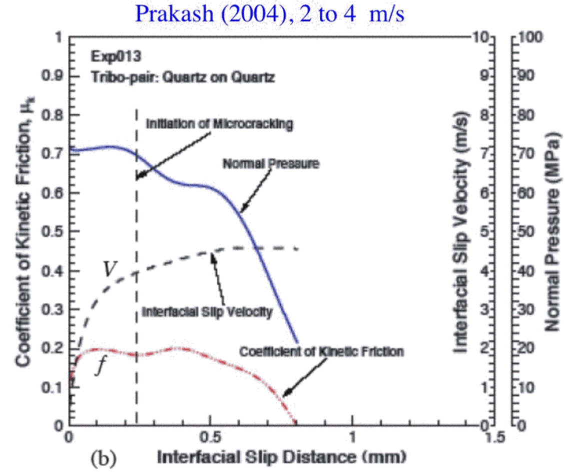

Pre-twisted torsional Kolsky bar (split Hopkinson bar) imposes slip at $V \sim$ 3-4 m/s, resulting in f slightly less than 0.2.

Experiment becomes uninterpretable after small slip (marked) due to cracking in wall of specimen.

Governing equations, 1-space-dimension shearing field, constant normal stress σ_n:

Thermal pressurization of pore fluid

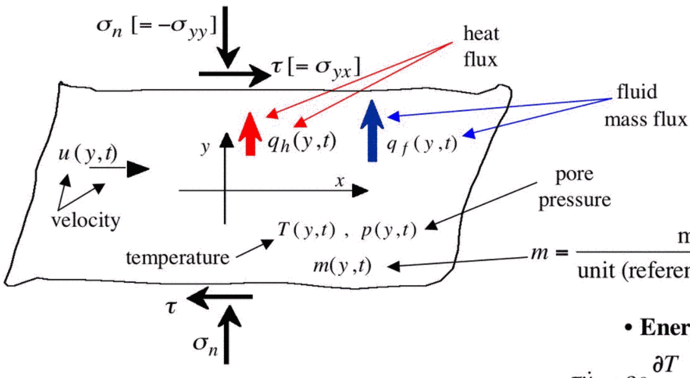

$$m = \frac{\text{mass of pore fluid}}{\text{unit (reference) vol. of porous medium}} = \rho_f n$$

• **Constitutive relation (for shear):**

$$\frac{\partial u}{\partial y} = \frac{\dot{\tau}}{\mu} + \dot{\gamma} \quad (\dot{\gamma} = \text{inelastic shear rate})$$

Friction law: $\tau = f \cdot (\sigma_n - p)$ if $\dot{\gamma} \neq 0$ ($\dot{\gamma} \geq 0$).

• **Equations of motion (= equilibrium equations):**

$$\frac{\partial \sigma_{yy}}{\partial y} = 0 \quad , \quad \frac{\partial \sigma_{yx}}{\partial y} = 0$$

$$\Rightarrow \quad \sigma_n \equiv -\sigma_{yy} = \text{const.} \; , \quad \tau \equiv \sigma_{yx} = \tau(t)$$

• **Energy equation:**

$$\tau\dot{\gamma} = \rho c \frac{\partial T}{\partial t} + \frac{\partial q_h}{\partial y} \; , \; q_h = -K \frac{\partial T}{\partial y};$$

$\rho c \approx 2.7$ MPa/ºC ; $\alpha_{th} = \frac{K}{\rho c} \approx 0.5\text{-}0.7 \text{ mm}^2/\text{s}$.

• **Fluid mass conservation:**

$$\frac{\partial m}{\partial t} + \frac{\partial q_f}{\partial y} = 0 \; , \; q_f = -\frac{\rho_f k}{\eta_f} \frac{\partial p}{\partial y} \quad \Rightarrow$$

$$\frac{\partial p}{\partial t} = \Lambda \frac{\partial T}{\partial t} - \frac{1}{\beta} \frac{\partial n^{pl}}{\partial t} + \alpha_{hy} \frac{\partial^2 p}{\partial y^2}; \quad \alpha_{hy} = \frac{k}{\eta_f \beta},$$

$\Lambda \approx 0.3\text{-}1.0$ (MPa/ºC), $\beta \equiv n(\beta_f + \beta_n) = 5.5\text{-}30 \times 10^{-11}$/Pa;

β_f, β_n = fluid compressibility, pore space expansivity.

A perspective on shear localization in fluid - infiltrated granular media

Assume that all inelastic dilatancy Δn^{pl} is over at small shear.

Then the governing equations for p and T are:

$$\frac{1}{\rho c} \tau(t) \dot{\gamma}(y,t) = \frac{\partial T}{\partial t} - \alpha_{th} \frac{\partial^2 T}{\partial y^2}$$

$$\Lambda \frac{\partial T}{\partial t} = \frac{\partial p}{\partial t} - \alpha_{hy} \frac{\partial^2 p}{\partial y^2} \; .$$

$$\tau(t) = f[\sigma_n - p(y,t)] \text{ if } \dot{\gamma}(y,t) \neq 0$$

Question: What type of solutions exist, if we assume that f = *constant*? Answer:

Either

(i) $p(y,t)$ is spatially uniform, $p(y,t) = p(t)$, $\Rightarrow T(y,t) = T(t)$, $\Rightarrow \dot{\gamma}(y,t) = \dot{\gamma}(t)$;
i.e., no fluid flow (*undrained*), no heat flow (*adiabatic*), homogeneous strain
(too idealized to be realistic, and has been proven
to be unstable to perturbations [Rice and Rudnicki, 2005]),

or

(ii) $\dot{\gamma}(y,t) = 0$ except at the isolated position(s) y where $p(y,t) =$ global maximum;
$\dot{\gamma}(y,t) = V(t)\delta_{Dirac}(y)$ for global max at $y = 0$ [$V(t) =$ slip rate].

Slip on a plane at slip rate V (Thickness h of shearing layer assumed small compared to boundary layers where p and T increase) :

- In $|y| > 0$, $\dfrac{\partial T}{\partial t} = \alpha_{th} \dfrac{\partial^2 T}{\partial y^2}$ and $\dfrac{\partial p}{\partial t} - \Lambda \dfrac{\partial T}{\partial t} = \alpha_{hy} \dfrac{\partial^2 p}{\partial y^2}$.
- On $y = 0^{\pm}$, $q_h = -K \dfrac{\partial T}{\partial y} = \pm \dfrac{f(\sigma_n - p)V}{2}$; $q_f = -\dfrac{\rho_f k}{\eta_f} \dfrac{\partial p}{\partial y} = 0$.
- Assumes all dilatancy Δn^{pl} (distributed) is over at small slip [$p_{amb} \rightarrow p_o = p_{amb} - \dfrac{\Delta n^{pl}}{\beta}$].

Simple solution : For $V \equiv d\delta / dt$ = constant, and f = constant, we solve for the fields $T(y,t)$ and $p(y,t)$, and hence $p(0,t)$, to evaluate $\tau = \tau(\delta) = f\left(\sigma_n - p(0,t)\right)$ (where slip $\delta = Vt$) :

$$\tau(\delta) = f(\sigma_n - p_o)\exp\left(\frac{\delta}{L^*}\right)\mathrm{erfc}\left(\sqrt{\frac{\delta}{L^*}}\right),$$

[Mase & Smith, 1987; Rice, 2005]

$$\text{where } L^* = \frac{4}{f^2}\left(\frac{\rho c}{\Lambda}\right)^2 \frac{\left(\sqrt{\alpha_{hy}} + \sqrt{\alpha_{th}}\right)^2}{V}.$$

Slip on a Plane, stress *vs*. slip (V= const.):

$$\frac{\tau}{f(\sigma_n - p_o)} = \exp\left(\frac{\delta}{L^*}\right)\mathrm{erfc}\left(\sqrt{\frac{\delta}{L^*}}\right) \; ; \; L^* = \frac{4}{f^2}\left(\frac{\rho c}{\Lambda}\right)^2 \frac{\left(\sqrt{\alpha_{hy}} + \sqrt{\alpha_{th}}\right)^2}{V} .$$

Note apparent multi-scale nature of the slip-weakening; no well-defined *Dc*:

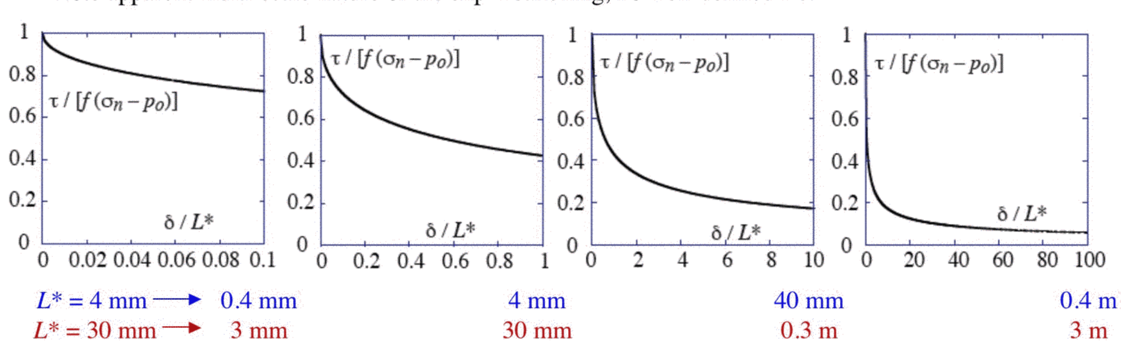

$$\text{On slip plane, } T - T_{amb} = \Delta T_{\max}\left[1 - \frac{\tau}{f(\sigma_n - p_o)}\right] , \; \Delta T_{\max} = \sqrt{\frac{f^2 V L^*}{4\alpha_{th}}}\,\frac{\sigma_n - p_o}{\rho c}$$

How large is L*?

$$L^* = \frac{4}{f^2}\left(\frac{\rho c}{\Lambda}\right)^2 \frac{\left(\sqrt{\alpha_{hy}} + \sqrt{\alpha_{th}}\right)^2}{V} .$$

Evaluations for 7 km depth, typical centroidal depth of crustal rupture zone;
$\sigma_n \approx$ overburden = 196 MPa, $p_o = p_{amb}$ = hydrostatic = 70 MPa, T_{amb} = 210 ºC:

Part of L^* based on poro-thermo-elastic properties of fault gouge:

Assuming relatively intact gouge, MTL properties

$$\left(\frac{\rho c}{\Lambda}\right)^2 \left(\sqrt{\alpha_{hy}} + \sqrt{\alpha_{th}}\right)^2 \approx \begin{cases} 60 \text{ mm}^2/\text{s (low end)} \Rightarrow L^* \approx 4 \text{ mm, if } V = 1 \text{ m/s and } f = 0.25. \\ 450 \text{ mm}^2/\text{s (high end)} \Rightarrow L^* \approx 30 \text{ mm, if } V = 1 \text{ m/s and } f = 0.25, \end{cases}$$

or $L^* \approx 50$ mm, if $V = 1$ m/s and $f = 0.20$.

Accounting approximately for ***damage*** at the rupture front and during subsequent shear, k^{dmg} = 5-10 k, β_d^{dmg} =1.5-2 β_d

[Rice, 2005]

• V = 1 m/s is the average ratio of *slip* to *slip duration* at a point, for the 7 slip inversions discussed in [Heaton, 1990], range is 0.56 to 1.75 m/s, average is 1.06 m/s).

• f = 0.25 represents effects of *flash heating*, like in *high-speed friction experiments* [Tullis and Goldsby, 2003; Prakash, 2004].

$\sigma_c - p$ (MPa)	$-\partial n / \partial \sigma_c$ $(= \beta_d - \beta_s)$ (10^{-11}/Pa)	β_d (10^{-11}/Pa)	n -	β_n^v (10^{-9}/Pa)	β_n^{el} (10^{-9}/Pa)	β_n^{dmg} (10^{-9}/Pa)	λ_n^{el} (10^{-4}/ºC)	k (10^{-20}m^2)	k^{dmg} (10^{-20}m^2)
160	3.0	4.6	[0.035]	0.84	0.55	2.2	−2.0	-	-
126	[4.22]	[5.82]	[0.04]	[1.04]	[0.65]	[2.49]	[−1.9]	0.65	6.5
120	-	-	-	-	-	-	-	[0.73]	7.3
100	[5.0]	6.6	0.042	1.2	0.72	2.7	−1.9	-	-
75	-	-	-	-	-	-	-	[1.5]	15
55	8.0	9.6	[0.050]	1.6	0.91	3.5	−1.8	-	-
50	[10]	12	0.055	1.8	1.0	3.9	−1.6	-	-
10	23	25	0.072	3.2	1.7	6.6	−1.3	[19]	190

Table 1: Properties of the ultracataclastic, clayey gouge containing the principal slip surface of the Median Tectonic Line fault zone, Japan. Results from Wibberley [2002] and private communication [2003], for pore compressibility parameter $-\partial n / \partial \sigma_c$ $(= \beta_d - \beta_s$; where β_d is drained bulk compressibility of the porous medium and β_s is compressibility of its solid grains) and for n (≈ porosity; precisely, the void volume per unit reference state volume of the porous aggregate). Results from Wibberley and Shimamoto [2003] in their Figure 8.b.ii provide permeability k; the value shown here at effective confining stress $\sigma_c - p$ = 126 MPa corresponds to their results for isotropic virgin consolidation to that confining stress. Their gouge was instead consolidated further, to $\sigma_c - p$ = 180 MPa, and then studied at various states of unloading (unloading and reloading are then approximately reversible) to provide the results in their Figure 8.b.ii. Permeability values k shown here are estimated values for an unloading curve starting at 126 MPa, assuming that at any given effective stress, the ratios of permeability along that curve, to those along the actually documented curve for unloading from 180 MPa, are in the same 1.91 ratio as the ratio of the virgin consolidation k (0.65×10^{-20}m^2) at 126 MPa to the k (0.34×10^{-20}m^2) at that same 126 MPa along the unloading curve from virgin consolidation to 180 MPa. Numbers in brackets are interpolated or extrapolated. Parameters β_n and λ_n enter an expression of type $dn = n(\beta_n dp + \lambda_n dT)$ characterizing effect of variation of pore pressure p and temperature T at various external constraints. Explanation of superscripts on β_n and λ_n: "v" is for variation at fixed confining stress σ_c; "el" and "dmg" are for variation at fixed fault-normal stress σ_n and zero fault-parallel strains, with "el" for elastic response of fault wall and "dmg" to approximately represent a damaged wall state with inelastic response for which, for the values shown here, β_d has been doubled, i.e., $\beta_d^{dmg} = 2.0\beta_d$. For that damaged state, the permeability k^{dmg} has been increased to 10 times k. For calculations of the table, the following values have been assumed: $\beta_s = 1.6 \times 10^{-11}$/Pa; solid grains volumetric thermal expansion $\lambda_s = 2.4 \times 10^{-5}$/ºC ($\lambda_n^v = \lambda_n^{dmg} = \lambda_s$); drained Poisson ratio of aggregate $\nu_d = 0.20$.

Models considered:	Intact Elastic Walls Ambient p and T	Intact Elastic Walls Average on p-T path	Highly Damaged Walls Ambient p and T	Highly Damaged Walls Average on p-T path
Common parameters assumed for all models:				
Specific heat of fault gouge [L], [VS], ρc (MPa/°C)	2.7	2.7	2.7	2.7
Starting porosity [W], n	0.04	0.04	0.04	0.04
Friction coefficient [flash heating, see text], f	0.25	0.25	0.25	0.25
Slip rate [see text], V (m/s)	1.0	1.0	1.0	1.0
Normal stress, σ_n (MPa)	196	196	196	196
Path ranges used for property evaluations:				
Pore fluid pressure range p_{amb}, p_{high} (MPa)	70, 70	70, 133	70, 70	70, 133
Effective stress range $\sigma_n - p_{amb}$, $\sigma_n - p_{high}$ (MPa)	126, 126	126, 63	126, 126	126, 63
Temperature range T_{amb}, T_{high} (°C)	210, 210	210, 334	210, 210	210, 810
Material properties (averages over path ranges):				
Thermal diffusivity [VS], α_{th} (mm^2/s)	0.70	0.65	0.70	0.50
Fluid thermal expansivity [B], λ_f (10^{-3}/°C)	1.08	1.21	1.08	2.30
Pore space thermal expansivity, λ_n (10^{-3}/°C)	−0.19	−0.18	0.02	0.02
Fluid compressibility [B], β_f (10^{-9}/Pa)	0.64	0.74	0.64	4.47
Pore space pressure expansivity [W], β_n (10^{-9}/Pa)	0.65	0.77	2.49	2.95
Fluid viscosity [K] [T], η_f (10^{-4}Pa-s)	1.48	1.26	1.48	0.77
Permeability [WS], k (10^{-20}m^2)	0.65	1.38	6.5	13.8
Resulting material properties:				
Undrained pressurization factor, Λ (MPa/°C)	0.98	0.92	0.34	0.31
Hydraulic diffusivity, α_{hy} (mm^2/s)	0.86	1.81	3.52	6.04
Resulting parameters of slip-on-plane model:				
Weakening length parameter, L^* (mm)	1.51	2.55	29.8	49.5
Maximum possible temperature rise, ΔT_{max} (°C)	271	366	1,200	1,840
Maximum possible T, T_{max} (°C) (for T_{amb} = 210 °C)	481	576	1,410	2,050

Table 2: Assumed and resulting parameters of the slip-on-plane model, to represent a mature fault surface at 7 km depth, at normal stress of 196 MPa, ambient pore pressure of 70 MPa, and ambient temperature of 210 °C. "Intact Elastic Walls" models use laboratory-constrained data for permeability k and pore space pressure expansivity $\beta_n = \beta_n^{el}$ of undisturbed gouge, and "Highly Damaged Walls" models account approximately but arbitrarily for gouge damage at the rupture front, and during slip and thermal pressurization, by using a differently defined pore space pressure expansivity $\beta_n = \beta_n^{dmg}$ and increasing k by 10× and β_d by 2× the laboratory-constrained values; k and the two β_n measures are assumed to vary only with $\sigma_n - p$. Fluid and other T or T-p dependent properties are evaluated as averages along straight line paths from p_{amb}, T_{amb} to p_{high}, T_{high}. The "high" values are set to ambient values in the 1st and 3rd columns. Results there are used to approximately estimate the p_{high}, T_{high} for the 2nd and 4th columns, respectively, as rough spatial averages, over the part of the wall that is actively participating in the heat and mass transfer, at the stage when p at the fault has been elevated to σ_n. Codes: B: Burnham et al. [1969]; K: Keenan et al. [1978]; L: Lachenbruch [1980]; T: Todheide [1972]; VS: Vosteen and Schellschmidt [2003]; W: Wibberley [2002] and private communication [2003]; WS: Wibberley and Shimamoto [2003]. Fluid properties estimated from B, K and T with the collaboration of Dr. A. Rempel.

Relation of fracture energy to slip weakening properties:

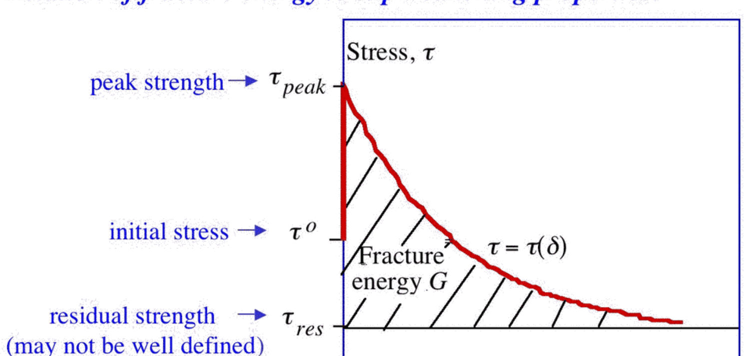

General definition of fracture energy associated with slip weakening on a fault:

$$G \equiv \int_0^{\delta_{\text{large}}} [\tau(\delta') - \tau_{res}]d\delta' \qquad \left(\tau(\delta_{\text{large}}) \approx \tau_{res}\right).$$

When a uniform residual level τ_{res} has *not* been reached at maximum slip δ, a consistent definition is:

$$G = G(\delta) \equiv \int_0^{\delta} [\tau(\delta') - \tau(\delta)]d\delta' .$$

Does ***not*** include contributions to G from inelastic deformation near the fault plane. How large?

Slip on a Plane, energy release rate

$$G = G(\delta) = \int_0^{\delta} [\tau(\delta') - \tau(\delta)]d\delta' = f(\sigma_n - p_o)L^* \left[\exp\left(\frac{\delta}{L^*}\right)\operatorname{erfc}\left(\sqrt{\frac{\delta}{L^*}}\right)\left(1 - \frac{\delta}{L^*}\right) - 1 + 2\sqrt{\frac{\delta}{\pi L^*}}\right]$$

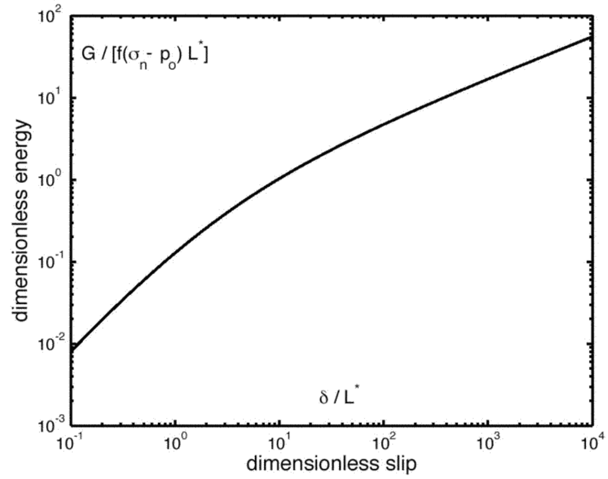

For $\frac{\delta}{L^*} >> 1$, $G \rightarrow 2(\sigma_n - p_o)\left(\frac{\rho c}{\Lambda}\right)\left(\sqrt{\frac{\alpha_{th} t}{\pi}} + \sqrt{\frac{\alpha_{hy} t}{\pi}}\right)$ (indep. of f and V! -- t = slip duration)

Seismic estimates of fracture energy (G):

Method A ***Use of seismic slip inversion results for large sets of earthquakes:***

A.1: Rice, Sammis and Parsons (*BSSA*, 2005), fit of seismic slip inversion results from Heaton (PEPI, 1990) to a steady state, self-healing, slip pulse model

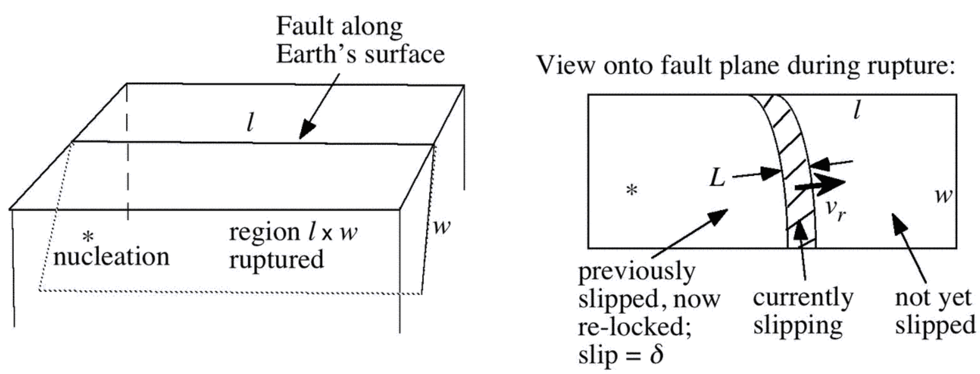

A.2: Tinti, Spudich and Cocco (*JGR,* in press 2005), use of kinematic slip (δ) inversions, smoothed, to get stress (τ) histories too, then use of

$$G = \int_0^{\delta} \left(\tau(\delta') - \tau(\delta)\right)d\delta'$$

Fracture energies G and slips δ, large earthquakes (arranged in order of slip magnitude)

Event	M_o 10^{18} Nm	l km	w km	δ m	G MJ/m^2	Ref.
Michoacan 1985 (M=8.1)	1,500	150	120	2.8	6.6	[1]
Landers 1992 (M=7.1)	56	60	14	2.2	5.0	[3]
Landers 1992 (M=7.3)	97	79	15	2.2	17.4	[2a]
San Fernando 1971 (M=6.5)	7	12	14	1.4	6.9	[1]
Northridge 1994 (M=6.7)	12	18	24	0.99	5.2	[2b]
Borah Peak 1983 (M=7.3)	23	40	20	0.96	2.9	[1]
Tottori 2000 (M=6.8)	13	29	18	0.80	3.7	[2c]
Kobe 1995 (M=6.9)	22	48	20	0.78	1.5	[4]
Kobe 1995 (M=6.9)	24	60	20	0.62	1.7	[2d]
Imperial Valley 1979 (M=6.5)	5	30	10	0.56	1.3	[1]
Imperial Valley 1979 (M=6.6)	7.7	35	12	0.6	0.81	[5]
Imperial Valley 1979 (M=6.6)	8.6	42	11	0.6	1.8	[2e]
Morgan Hill 1984 (M=6.2)	2.1	20	8	0.44	2.0	[1]
Morgan Hill 1984 (M=6.3)	2.7	30	10	0.26	2.0	[6]
Morgan Hill 1984 (M=6.3)	2.6	30	10	0.25	1.4	[2f]
Colfiorito 1997 (M=5.9)	0.71	10	7	0.38	0.83	[2g]
N. Palm Springs 1986 (M=6.0)	1.8	18	10	0.33	0.15	[1]
Coyote Lake 1979 (M=5.9)	0.35	6	6	0.32	0.57	[1]

[1] Rice, Sammis and Parsons [2005] based on slip inversions by Heaton [1990]. The G values are averages of G_{min} and G_{max} (= 2 G_{min}) of Rice et al. [2005]; i.e., $G = 1.5\, G_{min} = 0.75\, G_{max}$
[2] Tinti, Spudich and Cocco [2005]. [a] Avg. of 2 models, G values +/–16% of mean; [b] Avg. of 2 models, G values +/–11% of mean. [c] Avg. of 4 models, of which one is an average of 3 models, G values +92% to –54% of mean. [d] Single model. [e] Avg. of 2 models, G values +/–3% of mean. [f] Single model. [g] Avg. of 3 models, G values +34% to –52% of mean.

Seismically inferred fracture energies G *vs*. slips δ, large earthquake data set, compared to predictions of the thermal pressurization model for slip on a plane

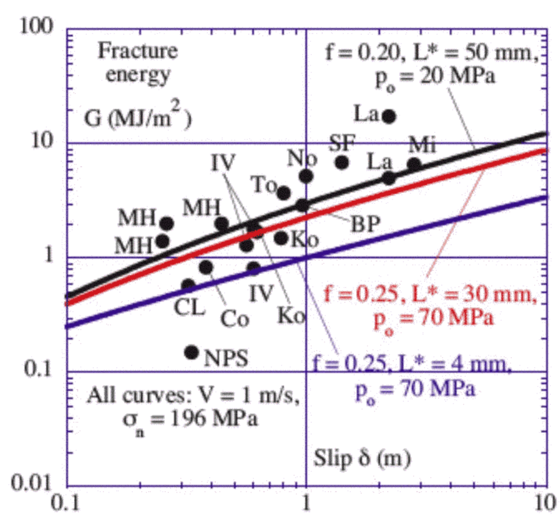

Method B (Abercrombie and Rice, *GJI*, 2005),
Use of radiated energy, moment, and source area (hence stress drop and slip):

Notation :

E_s = radiated seismic energy $\left(\int_S \int_0^\infty \rho (du/dt)^2 dt dS \right)$

A = rupture area (from corner frequency or duration)

δ = final slip (from moment $M_o = \mu\delta A$)

δ' = variable slip as event develops

τ_0 = initial shear stress

τ_1 = final static shear stress (stress drop $\tau_0 - \tau_1 \propto \mu\delta / \sqrt{A}$)

$\tau(\delta)[= \tau_{dyn}]$ = stress in last increment of dynamic slip

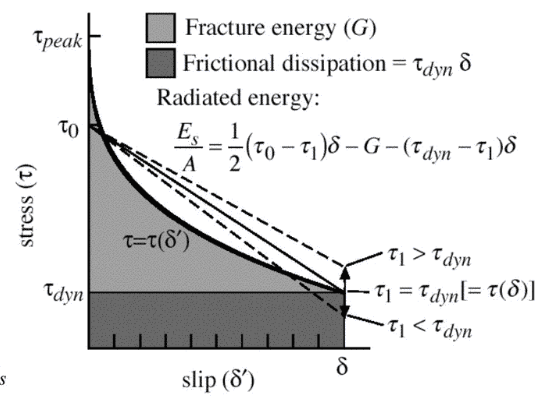

Energy balance :

$$\left(\frac{\tau_0 + \tau_1}{2}\delta\right) A = \left(\int_0^\delta \tau(\delta')d\delta'\right) A + E_s = \left(G + \tau_{dyn}\delta\right) A + E_s$$

$$\left(\text{since } G = \int_0^\delta [\tau(\delta') - \tau(\delta)]d\delta' = \int_0^\delta [\tau(\delta') - \tau_{dyn}]d\delta'\right)$$

$$\Rightarrow \frac{\tau_0 - \tau_1}{2}\delta = G + (\tau_{dyn} - \tau_1)\delta + \frac{E_s}{A}, \text{ or}$$

$$G' \equiv G + (\tau_{dyn} - \tau_1)\delta = \left[(\tau_0 - \tau_1) - \frac{2\mu E_s}{M_o}\right]\frac{\delta}{2}\ ;\ G' \approx G \text{ and } G' = G \text{ if } \tau_{dyn} = \tau_1$$

[We find, with the Madariaga (1979) estimate of $\tau_0 - \tau_1$, that $\mu E_s / M_o \approx 0.1(\tau_0 - \tau_1)$.]

Abercrombie (*JGR*, 1995) events, including Hauksson (*JGR*, 2000) focal mechanisms
[Abercrombie and Rice (*GJI*, 2005)]

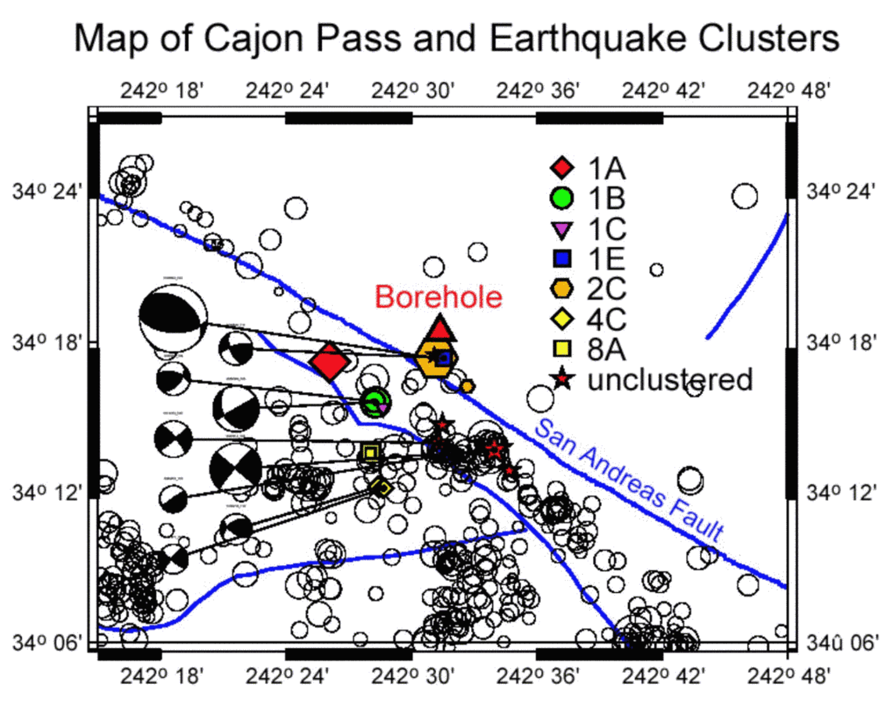

Comparison, predictions of *G* from the slip on a plane model with seismic estimates, for:

- **The large earthquake data set for *G* from seismic slip inversions for 12 events (shown as ovals here, one symbol per event),** ***and***

- **A data set for *G*' for small and large events based on radiated energy, moment, and seismic source dimension [Abercrombie & Rice, 2005]; *G*' ≈ *G*, and *G*' = *G* if stress during last increments of slip = final static stress after rupture (no overshoot/undershoot).**

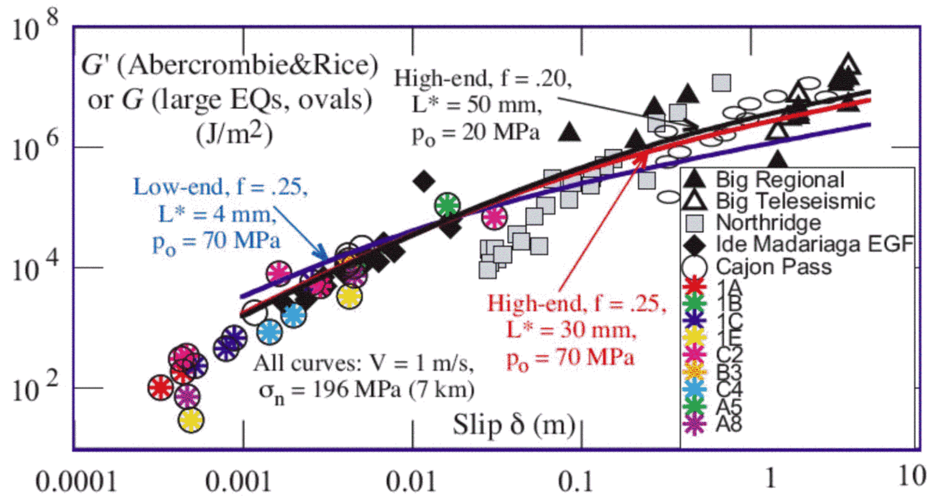

(Rice & Rudnicki, in progress, 2005)

Configurational stability of spatially uniform, adiabatic, undrained, shear:
(*Motivation:* Why do zones of localized slip have the thickness that they do?)

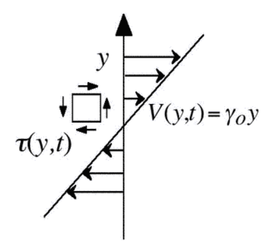

Governing equations for shearing velocity $V(y, t)$, ***shear stress*** $\tau(y, t)$, ***pore pressure*** $p(y, t)$, ***and temperature*** $T(y, t)$:

$$\frac{\partial \tau}{\partial y} = 0 \ \text{(inertia irrelevant)}, \ \sigma_n = \text{const.}$$

$$\tau = f(\partial V / \partial y)(\sigma_n - p), \ f'(...) > 0$$

$$\tau \frac{\partial V}{\partial y} = \rho c \frac{\partial T}{\partial t} + \frac{\partial q_h}{\partial y}, \ q_h = -\rho c \alpha_{th} \frac{\partial T}{\partial y}$$

$$\frac{\partial m}{\partial t} \equiv \rho_f \beta \left(\frac{\partial p}{\partial t} - \Lambda \frac{\partial T}{\partial t} \right) = -\frac{\partial q_f}{\partial y}, \ q_f = -\rho_f \beta \alpha_{hy} \frac{\partial p}{\partial y}$$

Simple ***rate-strengthening*** friction model; approximately valid only in *stable* regions in which rupture cannot nucleate, but may propagate through (or in *unstable* regions that have *shear-heated* to a frictionally stable *T* range).

(Fuller rate-state description, with *localization limiter*, must be used in regions of *unstable, rate-weakening*, friction.)

The spatially uniform solution:

$$V(y,t) = V_0(y) = \gamma_o y \quad (\gamma_o = \text{uniform shearing rate}),$$

$$p(y,t) = p_0(t), \ \tau(y,t) = \tau_0(t) = f(\gamma_o)[\sigma_n - p_0(t)],$$

$$\sigma_n - p_0(t) = [\sigma_n - p_0(0)]\exp(-H\gamma_o t) \ \ [\textit{call this } \bar{\sigma}_0(t)]$$

$$\text{where } H \equiv \frac{f(\gamma_o)\Lambda}{\rho c} \approx 0.1\text{-}0.3 f(\gamma_o),$$

$$T(y,t) = T_0(t), \ \rho c dT_0(t)/dt = f(\gamma_o)\bar{\sigma}_0(t)\gamma_o$$

Linearized perturbation about time-dependent spatially uniform solution:

$$V(y,t) = \gamma_o y + V_1(y,t)\ ,\ \ p(y,t) = p_0(t) + p_1(y,t)\ ,$$
$$T(y,t) = T_0(t) + T_1(y,t)\ ,\ \ f = f(\gamma_o) + f'(\gamma_o)\partial V_1(y,t)/\partial y$$

$$\frac{\partial}{\partial y}\left(-f(\gamma_o)p_1 + f'(\gamma_o)\frac{\partial V_1}{\partial y}\bar{\sigma}_0(t)\right) = 0$$

$$f(\gamma_o)\bar{\sigma}_0(t)\frac{\partial V_1}{\partial y} - f(\gamma_o)p_1\gamma_o + f'(\gamma_o)\frac{\partial V_1}{\partial y}\bar{\sigma}_0(t)\gamma_o = \rho c\left(\frac{\partial T_1}{\partial t} - \alpha_{th}\frac{\partial^2 T_1}{\partial y^2}\right)$$

$$\frac{\partial p_1}{\partial t} - \Lambda\frac{\partial T_1}{\partial t} = \alpha_{hy}\frac{\partial^2 p_1}{\partial y^2}$$

Nature of solution with spatial dependence $\exp(2\pi i y/\lambda)$***:***

$$\bar{\sigma}_0(t)\frac{\partial V_1(y,t)}{\partial y}\ ,\ \ p_1(y,t)\ ,\ \ T_1(y,t)\ \ \propto\ \ \exp(st)\exp(2\pi i y/\lambda)$$

$$\bar{\sigma}_0(t)\ \propto\ \exp(-H\gamma_o t)\ \Rightarrow\ \frac{\partial V_1(y,t)}{\partial y}\ \propto\ \exp[(s + H\gamma_o)t]\exp(2\pi i y/\lambda)$$

$s = s(\lambda)$ ***satisfies:***

$$zH\gamma_o s = \left(s + \frac{4\pi^2\alpha_{th}}{\lambda^2}\right)\left(s + \frac{4\pi^2\alpha_{hy}}{\lambda^2}\right) \quad \text{where} \quad z = \frac{f(\gamma_o)}{\gamma_o f'(\gamma_o)} = \frac{f}{a-b} \approx \frac{0.6}{0.015} = 40$$

Condition for linear instability of flow profile $\left(\frac{\partial V_1}{\partial y} \to \infty\right)$***:***

$$\mathrm{Re}(s) + \frac{f\Lambda}{\rho c}\gamma_o > 0 \ \ \Rightarrow\ \ \lambda > \lambda_{cr} \equiv 2\pi\sqrt{\frac{(\alpha_{th} + \alpha_{hy})\rho c}{(z+2)f\Lambda\gamma_o}}$$

For shear of layer of thickness h $\left(\gamma_o = \frac{V}{h}\right)$: $\quad \lambda > \lambda_{cr} \equiv 2\pi\sqrt{\frac{(\alpha_{th} + \alpha_{hy})\rho c h}{(z+2)f\Lambda V}}$

[Comment: Near $\lambda = \lambda_{cr}$, $\mathrm{Im}(s) \approx z\frac{f\Lambda}{\rho c}\frac{\sqrt{\alpha_{th}\alpha_{hy}}}{\alpha_{th} + \alpha_{hy}}\frac{V}{h}$ (oscillatory; unloading?)]

Possible self - consistent estimate of shear layer thickness h at large shear :

$$\text{Set } \gamma_o = \frac{V}{h},\ \lambda_{cr} \approx h \ \Rightarrow\ h \approx \frac{4\pi^2(\alpha_{th} + \alpha_{hy})\rho c}{(z+2) f \Lambda V}$$

Results (using $z = 40$, $V = 1$ m/s, $\alpha_{th} = 0.7$ mm^2/s, $\rho c = 2.7$ MPa/ºC):

Low end ($\Lambda = 0.70$ MPa/ºC, $\alpha_{hy} = 1.5$ mm^2/s): $h = 4.4$ µm / $f = 11$ µm (if $f = 0.4$).

High end ($\Lambda = 0.34$ MPa/ºC, $\alpha_{hy} = 3.5$ mm^2/s): $h = 31$ µm / $f = 78$ µm (if $f = 0.4$).

Implications:

- Even with *velocity strengthening* [with large z (= f / [$\gamma\, df/d\gamma$]), e.g., of order $z > 10$], we must expect large shear strain to be confined to a thin zone, less than diffusion penetration distances of heat and fluid in moderate and larger events.

- Justifies use of model based on slip on a plane.

- Observed 1-5 mm deformed zone thickness in gouge may be a *precursor* thickness (i.e., λ_{cr} based on an initial, broad h) *not* the thickness of the large shear zone.

Silica gel (?) formation

Weakening in large and moderately rapid ($V \geq 1$ mm/s) slip, in rocks of high silica content, in presence of water.
[Goldsby & Tullis, *GRL* 2002; Di Toro, Goldsby & Tullis, *Nature* 2004; Roig Silva, Goldsby, Di Toro & Tullis, *EOS* 2004]

Quartzite (novaculite) experiments, oscillating shear of rotating annuli, results smoothed for reversal effects:

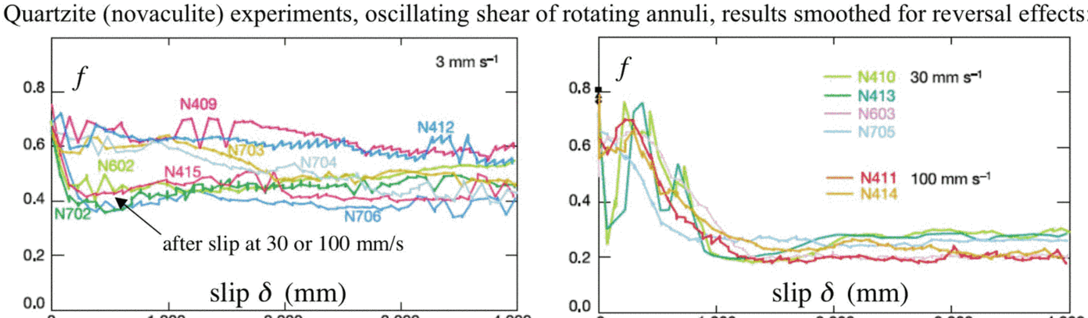

Susceptibility to weakening and ***silica content*** are ordered the same:
quartzite (Arkansas novaculite) > granite (Westerly) ≈ feldspar (Tanco albite) > gabbro
[high weakening, as above] [~none]

Slip surface morphologies which showed [Tulllis, priv. comm. 2004] "*now solidified … flow-like textures that make it … evident that at the time the deformation was going on, a thin layer coating the sliding surface was able to flow with a relatively low viscosity*". Such "*solidified flow structures have so far only been seen for novaculite*".

Otsuki, Monzawa & Nagase, *J. Geophys. Res.* (2003)

OTSUKI ET AL.: FLUIDIZATION AND MELTING OF FAULT GOUGE ESE

The melting range
-- some pictures

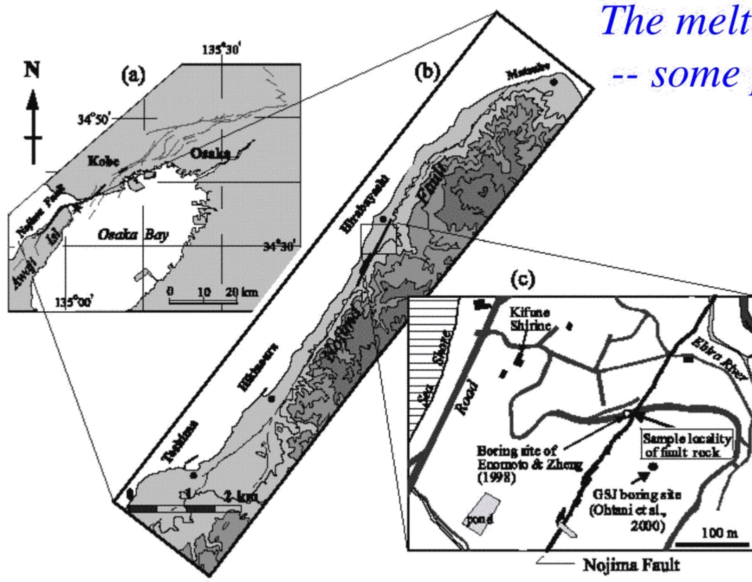

Figure 1. Active faults in the Kobe-Osaka area (thin lines) including the surface trace of the seismic Nojima fault (thick line), and sampling locality of the fault rocks studied in this paper.

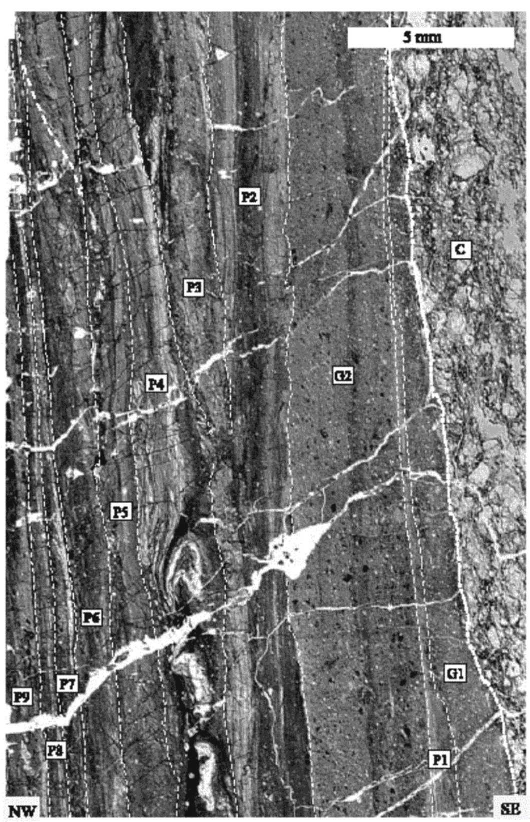

Otsuki, Monzawa & Nagase, Fluidization and melting of fault gouge, *J. Geophys. Res.* (2003):

Shear zones P1, …, P9: 9 pseudotachylyte-generating events (or fewer?):

- No or minimal overlap of shear zones P1, …, P9.
- All 9 shear zones fit within a 20 mm width.
- Individual zones have $h < 2$ mm, often < 1 mm. Suggests extremely localized shear prior to melting.

Figure 3. Photomicrograph of a thin section of thinly laminated fault rock. C: granitic cataclasite, G: fault gouge, and P: pseudotachylyte. Broken lines denote the boundaries between layers formed by different seismic slip events. A thick broken line in layer P6 indicates sinusoidal lamina.

data of A. Tsutsumi and T. Shimamoto,
High-velocity frictional properties of grabbro,
Geophys. Res. Lett., 24, 699-702, 1997

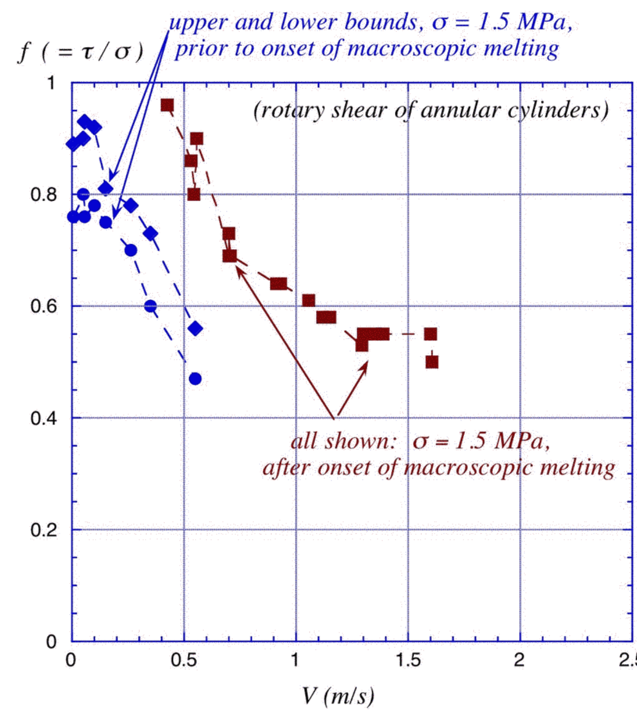

Melting does not necessarily weaken!

Various degrees of melting:

OTSUKI ET AL.: FLUIDIZATION AND MELTING OF FAULT GOUGE **ESE**

high melting

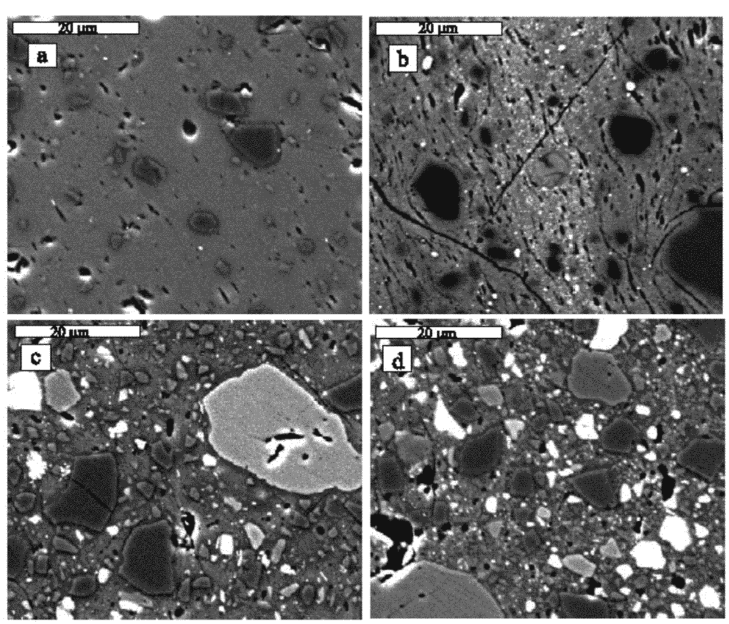

low melting

Figure 9. Backscattered electron images of pseudotachylyte samples showing various degrees of melting. a: volume fraction ϕ of ummelted grains = 0.08, b: $\phi = 0.119$, c: $\phi = 0.415$, and d: $\phi > 0.482$. Dark gray grains: quartz, gray grains: plagioclase, and white grains: potassium feldspar (large) and Fe-rich spherules (small). Elongated vesicles are well developed in a and b.

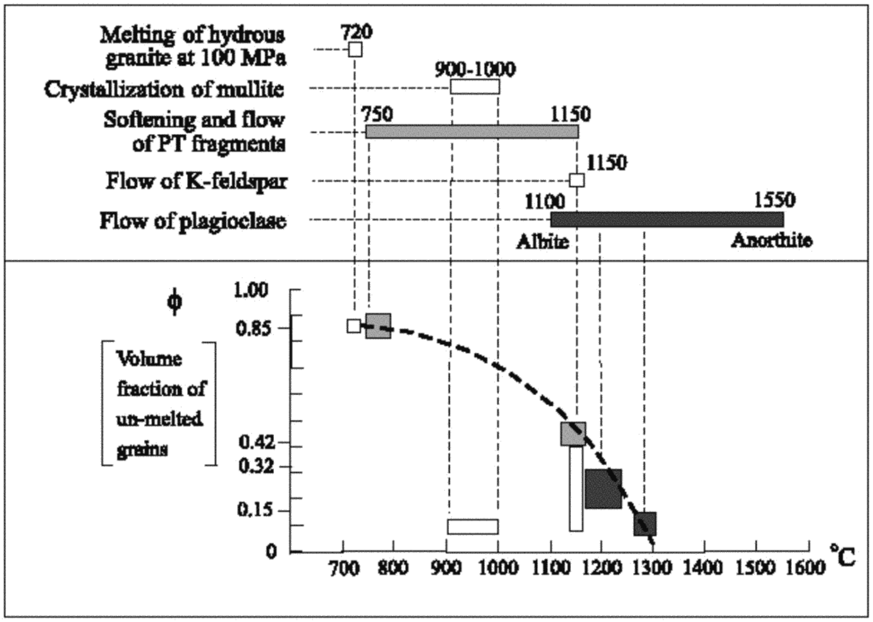

Figure 16. Various temperature indices (above) and the estimated temperature of pseudotachylyte melt as a function of the volume fraction ϕ of unmelted grains (below). Melting started at about 750°C, and the maximum temperature reached 1280°C.

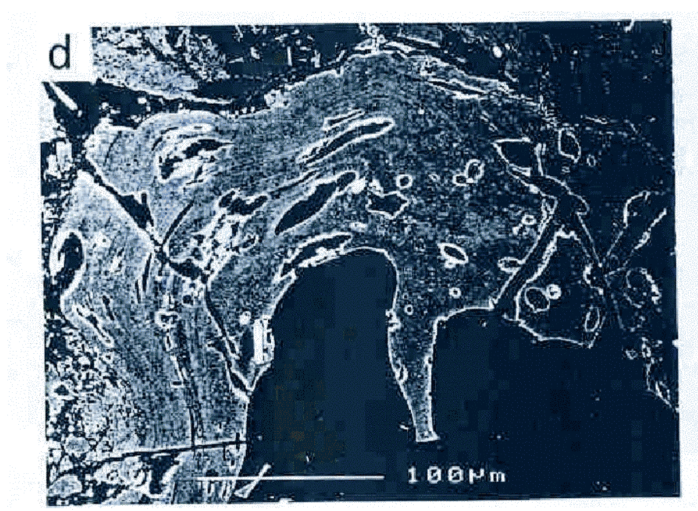

FIG. 1 – *BSE photomicrograph of an area of glassy pseudotachylyte in a sample from Outer Hebrides Thrust of the Western Isles, northwest Scotland. Taken from* Spray *[1993]*

Faults that are *statically strong*, but *dynamically weak*, can operate at *low overall stress*, and with *negligible heat outflow*, provided that "defect" regions Are present allow rupture nucleation (by concentrated τ, low σ_n, and/or elevated p). [Lapusta & Rice, 2004; Rice, 1996]

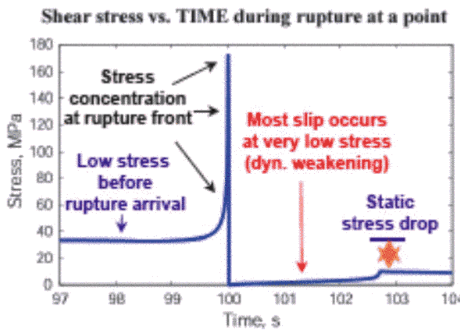

Shear stress evolution at a *statically strong* fault point during dynamic rupture

Static stress drop is *much smaller* than what one would expect *because* shear stress before the earthquake is much smaller than static strength.

Note:

In this case (L = 40 mm):
Static stress drop is ~20 MPa;
Slip is ~18 m.

Both would decrease for smaller L
(hard to resolve numerically for this V_w).

Pulse-like rupture propagation!

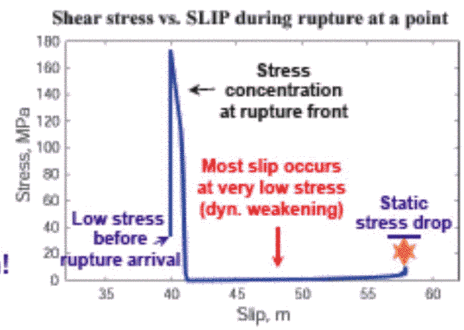

Conclusions :

• Mature crustal faults are likely to weaken during seismic slip by
  - *shear heating and thermal pressurization of pore fluid*

and by
  - *flash heating at frictional micro-asperity contacts.*

• The mechanisms are consistent with geological fault zone studies and with laboratory determinations of properties of fault-related materials.

• They predict fracture energies (G) in the broad range inferred seismically.

• Predictions have what seems to be an approximately correct scaling with earthquake slip over the entire range from a few mm to a few m.

• The mechanisms explain why melting does not generally occur at shallow to moderate depths, or may at least be delayed until unusually large slips.

- *Major questions:*

-What role for off-fault inelasticity? Are we misinterpreting seismically inferred *G*?

- What sets the thickness (*h*) of the zone of highly localized shear?

- What amount of dilatancy (Δn^{pl})?

-What is the pore expansivity (β_n) and permeability (*k*) for *damaged, inelastically deforming* gouge? -- and how to characterize such deformation and damage?

- What predictions to be made when such constitutive laws as derived here are used in dynamic rupture simulations?

- What rheology of the "liquefied" gouge resulting when $p \approx \sigma_n$? Is $\tau \approx 0$?

- What rheology if melting does begin? -- if transition to gel layer?